J. Integr. Sci. Technol. 2023, 11(4), 567 Article

Journal of Integrated
SCIENCE & TECHNOLOGY

Performance evaluation of FR2-based IoT and AI applications using a Quad Port Multiple Input Multiple Output Antenna

Kuldeep Pandey*, Ritesh Sadiwala

Department of Electronics and Communication, RKDF University, Bhopal. India.

Received on: 12-Apr-2023, Accepted and Published on: 05-Jun-2023

ABSTRACT

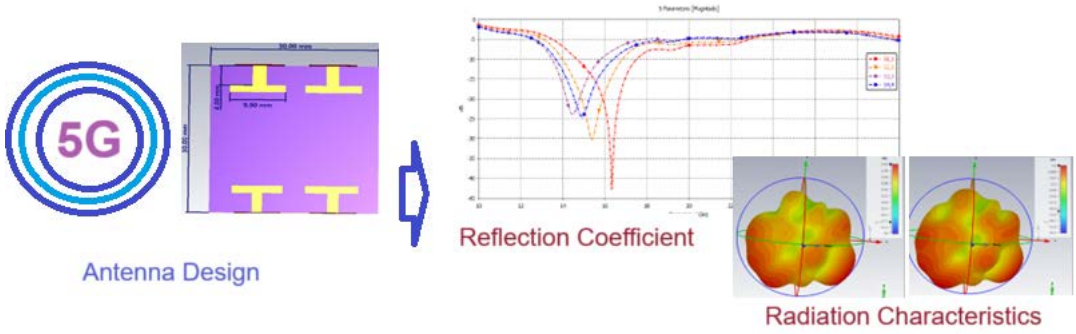

A four-port Multiple-Input-Multiple-Output (MIMO) antenna array with a rectangular slotted construction in the ground plane is utilized to improve the antenna's radiating capabilities. The suggested antenna features an FR4 substrate with 30x30 mm^2 measurements. The modeling and measurement results are found to be in good agreement. After that, a pattern is created and assessed. The highest peak gain of 5.03 dBi and performance characteristics of the suggested MIMO system make it suitable for deployment in 5G communication networks. The antenna's design has higher operating bands, an antenna array for greater gain, and a defined frequency range appropriate for 5G mm-wave communication. The radiation characteristics guarantee effective signal transmission and reception, resulting in increased network capacity and better user experience. Additionally, the use of an antenna array allows for beamforming, which enables targeted communication and reduces interference. With its robust design and excellent performance, the suggested MIMO system is poised to revolutionize 5G communication networks and meet the increasing demands of high-speed data transfer in the era of the Internet of Things (IoT) and connected devices.

Keywords: Antenna array; Defected Ground Structure (DGS), IoT, Multiple-Input-Multiple-Output (MIMO), 5G millimeter-wave

INTRODUCTION

The fifth generation of wireless technology is a reflection of connectivity growth. 5G, which was created for maximum speed and capacity, will make several new applications and use cases that go well beyond the smartphone conceivable. Engineers are already hard at work on the software and gadgets that will benefit from the advantages of 5G, even though widespread 5G rollouts are anticipated to happen in 2021.[1] The expansion of the IoT and substantial breakthroughs in the use of AI are two of the most intriguing technological developments of the future that will require 5G connectivity. Despite being up to 20 times faster than 4G, 5G offers much more than just quicker speeds. Programmers will be able to take advantage of 5G speeds and low latency by creating apps that include almost real-time video broadcasting for security or sporting events.[2] Additionally, 5G connectivity will make it feasible to have more real-time access to data from various solutions. Because they are energy-efficient and have a long lifespan, Internet of Things (IoT) sensors are employed by 5G. This would allow for remote monitoring of adjustments to irrigation levels and factory equipment conditions.[3] Doctors may have easier access to patient data that is secure. AI will be utilized to make each of these possibilities useful. The fastest broadband speed and least lag will soon be available to everyone in the world thanks to 5G technology. It must utilize three frequency bands (Sub-1 GHz, 1 to 6 GHz, and over 6 GHz are these bands) to operate properly and to fully cover and support all services offered by the preceding technology. Urban, suburban, and rural locations can all have extensive coverage thanks to the Sub-1 GHz band, which also supports the Internet of Things services. The 1-6 GHz band, however, provides advantages in terms of capacity and coverage.[4] Ultra-high broadband rates required for 5G can be delivered by the spectrum above 6 GHz. Urban, suburban,

*Corresponding Author: Kuldeep Pandey, Bhopal
Email: kuldeeppandey23@gmail.com

Cite as: *J. Integr. Sci. Technol., 2023, 11(4), 567.*

 ISSN: 2321-4635
http://pubs.thesciencein.org/jist

and rural areas can all have extensive coverage thanks to the utilization of the Sub-1 GHz band, which also allows Internet of Things services. The 1-6 GHz band, however, provides advantages in terms of capacity and coverage. Ultra-high broadband rates required for 5G can be delivered by the spectrum above 6 GHz. Many nations are considering, preparing for, or have already held an auction for the 3.5 GHz spectrum, as suggested by the Globally Mobile Suppliers Association (GSA). But millimeter wavebands starting at 24 GHz will be required to achieve the higher broadband speed requirement of up or around to 20 Gb/s.[5] The GSMA suggested that mobile devices use the 26 GHz operating bands (24.25 GHz-27.5 GHz), 40 GHz operating bands (37.5 GHz-43.5 GHz), and 67 GHz-71 GHz operating bands. As a result, licensing sales for the millimeter wave and 5G mid-band will take place in numerous nations over the following few years.[6] Combining unlicensed and licensed bands could help the operators further enhance the 5G user experience. In the 3.5 GHz unlicensed spectrum in light of this, the 5G mid-band may function at a frequency of 6 GHz, which is comparable to the 2.4 GHz and 5 GHz Wi-Fi frequencies. High data speeds are achieved using the 5 GHz frequency, whereas coverage is achieved using the 2.4 GHz spectrum.[7,8] The unlicensed 6 GHz spectrum may be utilized to deliver a higher data rate, while the 3.5 GHz band may be used to appropriate coverage and capacity, i.e., it will sustain the growing figure of users. Therefore, creating a patch antenna that resonates in these frequency bands will be advised.[9-12] Numerous operating mm-wave antenna solutions for 5G applications have recently been described in the existing literature.[13-22] The low-gain antenna designs now used in the possible mm-wave bands cannot handle the severe atmospheric and propagation losses associated with the mm-wave frequency.[23-25] Numerous higher gain value and beam-steering antenna array approaches have been proposed.[6-14] to reduce these effects of attenuation while maintaining strong signal strength and wide geographic coverage. However, because they are fed via a single port, multiple-element antenna arrays have the same capacity as a single antenna. MIMO antennas, which are essential to the development of 5G, exhibit multipath propagation with increased data speed, capacity, and connection reliability. Recent reports in the literature[15-26] have discussed a variety of MIMO antenna approaches for 5G mm-wave applications. The literature[15] describes a PIFA antenna array with a MIMO configuration that runs at 1 GHz and has the highest simulated gain of 12 dBi. A reference discusses a millimeter-wave MIMO antenna with a 0.8 GHz bandwidth. A multiple-element antenna design for 5G communications allows energy radiation to bend in the direction of a chosen inclination, according to reference. The antenna shape has a 1.5 GHz bandwidth between 27.2 GHz and 28.7 GHz with a maximum gain of 7.41 dBi at 28 GHz. DRA-based antennas for 5G applications have a constrained data rate of about 1 GHz, according to sources.[18,19] A larger gain of 7.37 is shown for the SIW feeding technique by Y. Sun et.al.[18] M.S. Sarawi et.al.[19] evaluated ECC as well to ensure MIMO performance. An SIW fed-slotted MIMO antenna array is also covered by B. Wang et.al.[20] The gain fluctuates between 8.2 and 9.6 dBi over the operational frequency range, and the suggested antenna supports the 5G bands at 24.25-27.5 GHz and 27.5-28.35 GHz. A four-element T-shaped MIMO antenna for 5G applications has overall dimensions of 12x50.8x0.8 mm^3.[21] The partial ground of the lower layer consists of symmetric split-ring slots arranged iteratively. The suggested antenna design has a peak gain of 10.6 dBi and a broad frequency range of 25.1-37.5 GHz. However, this paper just touches on ECC's performance in MIMO. An 8x8 MIMO antenna design with an overall substrate dimension of 31.2 x 31.2 1.57 mm^3 is shown by N. Shoaib et.al.[22] The proposed MIMO structure has a maximum gain of 8.732 dB, a maximum bandwidth of 5.68 GHz at -6 dB reference, and a resonance frequency of 25.2 GHz. It also considers the effects of diversity gain, MEG, and ECC. A two-port MIMO array has been made accessible for 5G communication systems.[23] Its dimensions are 31.7 x 53 x 0.2 mm^3 in total. The microstrip feedline receives the energy that is released. The disclosed antenna system with an EBG-based reflector offers a broad bandwidth and a high gain of up to 11.5 dB in the working spectrum. H. Jiang et.al.[24] additionally provided a 5G MIMO antenna with three pairs of connected metamaterial arrays and a study of ECC and Diversity gain for the suggested MIMO design. The substrate has an overall size of 30 x 30.5 x 0.58mm^3 and a maximum gain of 7.4 dBi at 26 GHz. A high-gain Fabry Perot antenna with a superstrate have also been included by Hussain et.al.[25] in study for 5G MIMO applications. The suggested structure operates with a maximum gain of 14.1 dBi in the mm-wave range between 26-29.5 GHz. To assess the MIMO performance of the current antenna design, ECC is also looked into. Y. Zhang et.al.[26] reported a two-element MIMO dielectric resonator antenna (DRA). For 5G applications, the reported antenna spans the band from 27.19 to 28.48 GHz. The result is an antenna with a gain of almost 10 dB. The TARC, ECC, DG, and channel capacity are also looked into.

In this work, a four-element MIMO antenna array for millimeter-wave 5G frequency ranges have been built. For developing 5th-generation devices like the Internet of Things, artificial intelligence, wearables, mobile Wi-Fi, etc., the proposed antenna achieved higher gain, multiple operating band antenna with good MIMO capabilities. Because of its compact size and simple design, the proposed MIMO antenna is simpler for 5G smart devices to include. The design's viability for impending 5G wireless communication applications is confirmed by the antenna's robust MIMO performance.

METHODOLOGY

MIMO antenna systems, which use multiple antennas for signal transmission and reception, are used in wireless communication to improve performance. Four antennas are used in this example's 4-port MIMO system, which can be used for several things, including enhancing signal quality, boosting data throughput, and lowering interference. Designing and analyzing electromagnetic structures, such as antennas, frequently uses CST Microwave Studio. A four-port MIMO (multiple-input, multiple-output) antenna system is used in this work. The recommended system was modeled using the CST Microwave Studio package, a commercial electromagnetic (EM) simulation software, and is built with precise substrate dimensions. According to reports, the antenna's substrate is 1.6 mm thick, 30 mm long, and 30 mm wide. The proposed MIMO antenna structure is shown on the top and bottom sides in Figure 1 using a Defected Ground Structure (DGS).

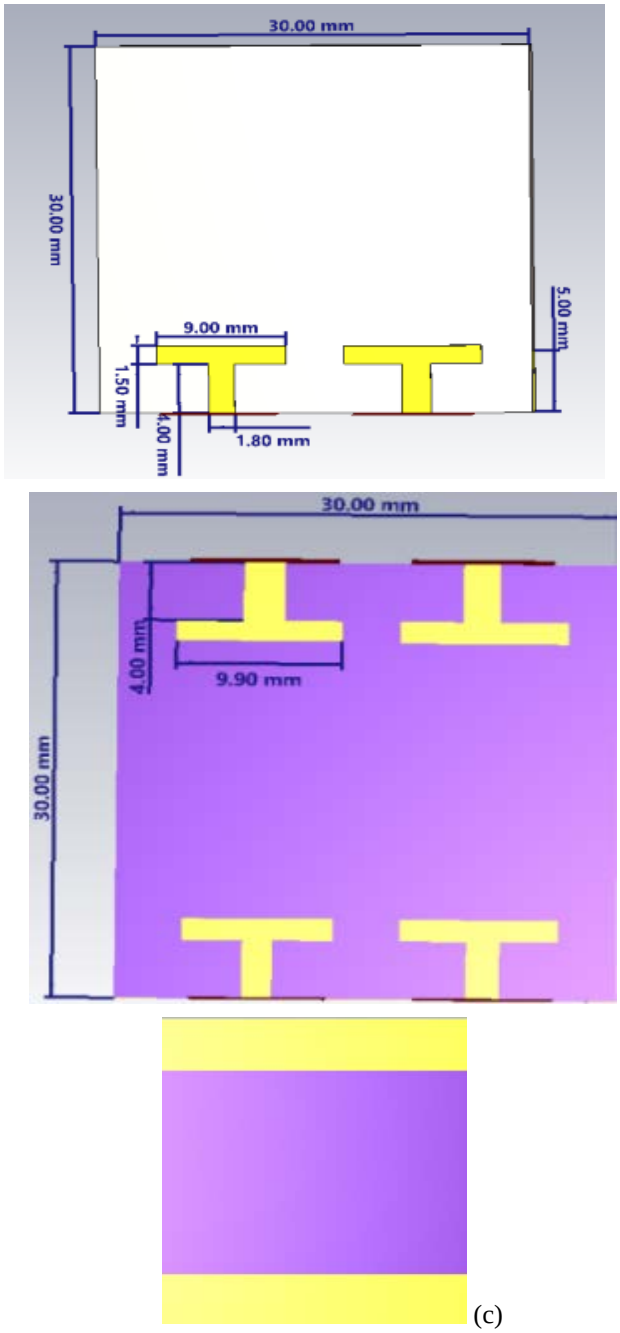

Figure 1: (a) Two Port Antenna Top view (b) Four Port Antenna Top view (c) Antenna Bottom view

Four MIMO elements compose the antenna system's configuration. Each of these components is positioned at the top and bottom of the radiating patch to create a geometric framework. The geographical distribution of the antennas is improved by this design and performance. The design has a defective ground structure (DGS) in the bottom layer. This method of designing antennas alters the ground plane to improve the performance of the antenna. To enhance specialized performance, rectangular slots are in this case incorporated into the ground construction. On a FR4 substrate, the antenna design is built. The substrate has a permittivity (r) of 4.4 and is 1.6 mm thick. An antenna's characteristics are influenced by the permittivity value, which also impacts an object's capacity to transmit electromagnetic waves swiftly. The study article examines how antenna designs evolved from having only one antenna element to having four elements in a MIMO arrangement. This includes looking at how the addition of various components affects elements like gain, radiation patterns, and impedance matching.

The behavior of the antenna characteristics was initially investigated using a two-port antenna (shown in Figure 1a), and the observed response was recorded in Figure 3. The formulas1-4[27–28] should be used to calculate the antenna's length and width.:

$$W = \frac{c}{2f_r}\sqrt{\frac{2}{\varepsilon_r + 1}} \quad (1)$$

$$L = \frac{c}{2f_r\sqrt{\epsilon_{reff}}} - 2\Delta L \quad (2)$$

$$\Delta L = 0.412h\,\frac{\varepsilon_{reff} + 0.3}{\varepsilon_{reff} - 0.258}\left[\frac{\frac{w}{h} + 0.264}{\frac{w}{h} + 0.8}\right] \quad (3)$$

$$\varepsilon_{eff} = \frac{\varepsilon_r + 1}{2} - \frac{\varepsilon_r - 1}{2}\left[1 + 12\frac{h}{w}\right]^{-\frac{1}{2}} \quad (4)$$

Where h is the height of the substrate, Wp and Lp are the width and length of the patch, and ε_{eff} and $\varepsilon_{relative}$ are the substrate's effective permittivity and relative permittivity, respectively. The formulas for the central frequency, effective length, and light speed are ΔL, fc, and c respectively.

The proposed excitation mechanism for the array is the parallel feed network. The branching network's impedance is matched at 100 Ω whereas the main feed's impedance is 50 Ω. As seen in Figures 2 and 3, the bottom layer is then added together with a collection of rectangular slots to further optimize the outcomes. As a result, the suggested antenna array has a greater bandwidth and gain. A wavelength separates the array antenna's two components. Thus, a small array construction with proven performance is achieved. A four-port MIMO antenna system was created using the architecture after the two-element array's success. The antenna array that was previously made serves as the foundation for each MIMO component in this system. These MIMO components are successfully positioned at the top and bottom of the board sides. The spatial distribution of the antennas is likely enhanced by this design. The 30 x 30 mm^2 board on which the designed MIMO antenna system is implemented has overall dimensions of 30 mm by 30 mm. These measurements are crucial for keeping the antenna parts and related structures contained. The performance of each antenna individually may be affected by interactions between two nearby array antennas. To improve the performance of the four-port MIMO antenna system and lessen mutual coupling among the antennas, a rectangular Defected Ground Structure (DGS) is added to the design. This DGS is precisely positioned to achieve the proper isolation between the MIMO antennas. Increased antenna isolation in the MIMO configuration is the intended outcome of including the rectangular-shaped DGS in the design. Improved isolation ensures that the antennas can operate with less interference from one another

for a reliable MIMO system to function. The material presented discusses the transition from a two-element array to a four-port MIMO antenna system, as well as the measures taken to enhance performance through strategic antenna placement and the implementation of a DGS structure to lessen mutual coupling. An iterative design methodology and the implementation of design enhancements offer a systematic method for optimizing MIMO antenna systems for improved overall performance.

RESULTS AND DISCUSSIONS

Analysis of Reflection Coefficients: Starting with a two-port element configuration and working up to a MIMO configuration, the antenna system's reflection coefficient curves are examined. The reflection coefficient measures how well the antenna matches the associated system's impedance. These curves aid in evaluating the antenna design's performance and resonance behavior.

The signal power from one antenna to another can be determined using the transmission coefficient curves in Figure 2. They are applied to measure the isolation between different antenna components of the MIMO framework. The study demonstrates that there are various degrees of isolation between various antenna pairs. Specifically: The isolation of antennas 1 and 2 is weak. Similar behavior is shown by antennas 3 and 4, indicating that a maximum observed isolation of -24.8 dB was attained. The couple's antenna 1 and 3, antenna 1 and 4, antenna 2 and 3, and antenna 2 and 4 all experience considerable isolation of -42.56 dB. The ground plane of the MIMO antenna structure now includes a rectangular Defected Ground Structure (DGS) in response to observations of low isolation between some antenna pairs. This DGS is designed to lessen the impacts of mutual coupling, a situation where the electromagnetic field of one antenna affects the performance of another. The DGS will be used to lessen this mutual coupling and enhance antenna separation. Measurements of the separation between the designed MIMO antennas reveal a minimum separation of less than -10 dB. This suggests that even if some coupling between certain antenna pairs is theoretically possible, design innovations like the use of DGS have been able to maintain a certain amount of isolation. Overall, the analysis emphasizes the need for effective MIMO antenna isolation to avoid interactions with surrounding antennas materially impairing the performance of each antenna. The rectangular-shaped DGS has been included to address mutual coupling difficulties and improve overall isolation between antennas in the MIMO array.

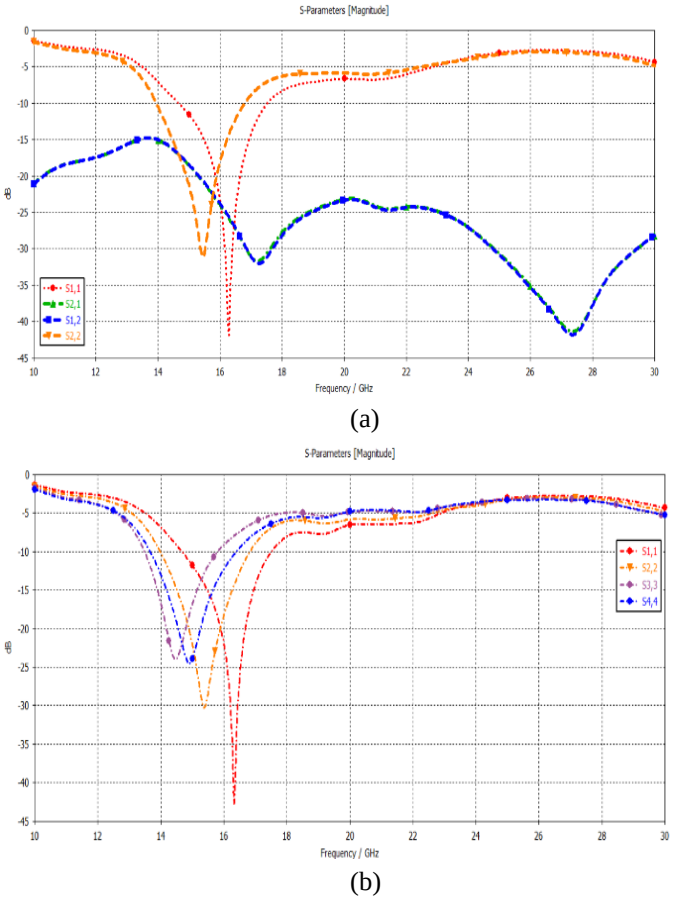

Figure 2. Simulated Reflection Coefficient of (a) Two Element, Designed Antenna (b) Reflection coefficient of Four Element MIMO antenna with DGS

Frequency Resonance: It has been found that the two components of the designed antenna resonate between 14.2 GHz and 16.8 GHz, which is the millimeter-wave frequency spectrum. The frequency range at which an antenna effectively receives or transmits signals is known as resonance. This frequency range appears to be compatible with the high data transfer efficiency mm-wave frequency spectrum.

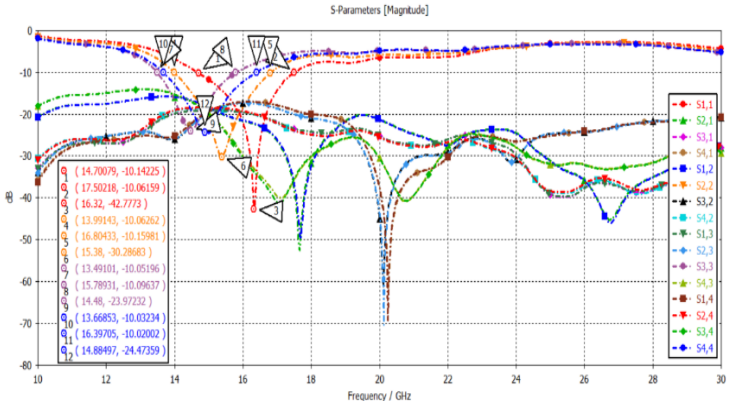

Figure 3. Reflection coefficient of Four Element MIMO with DGS (Simulated)

Increase in Bandwidth with Array Size: From a two-element array to a four-element array, the antenna design seems to increase the antenna bandwidth. The bandwidth of an antenna is the range of frequencies that it can successfully operate over. The increased bandwidth indicates that the antenna system can now cover a wider frequency range.

To understand the radiational behavior of the designed design, the 2D radiation patterns of antennas were investigated in an anechoic environment using the commercial ORBIT/FR far-field measuring device, as shown in Figure 4. The xz and yz planes were used for measurements in the far field with a theta bandwidth of -90° to 90°.

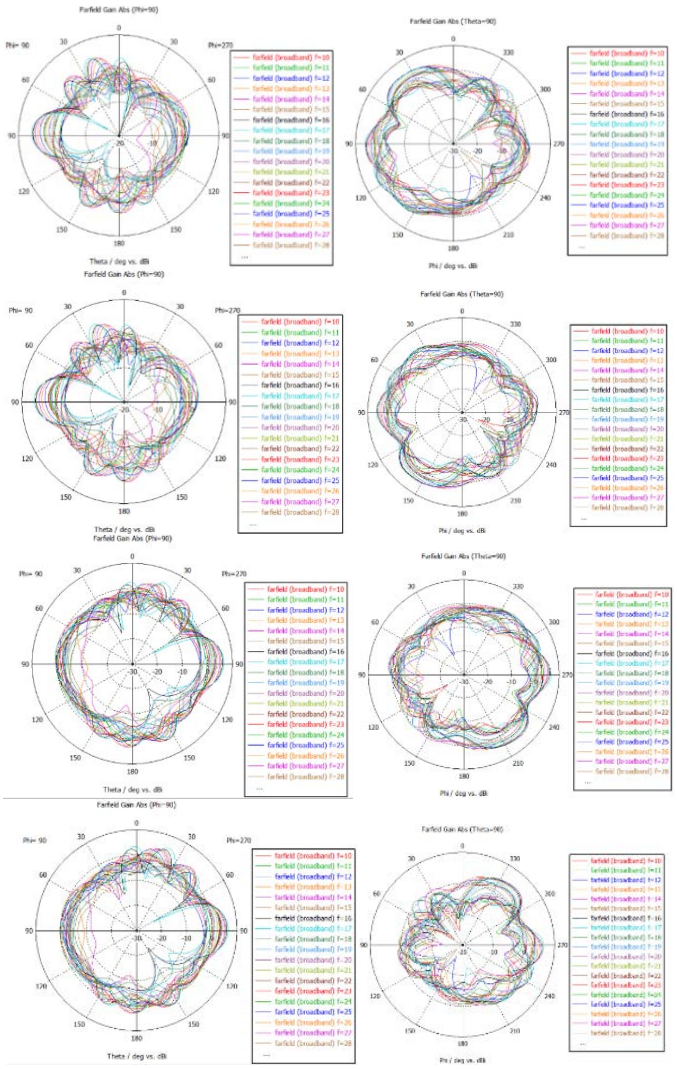

Figure 4. The Designed Antenna (Measured) Radiation Characteristics

A horn antenna with a typical gain of 20 dBi was used for signal transmission. Figures 4 and 5 depict the calculated and measured 2-D and 3-D radiation patterns of a four-element antenna. Both in models and in actual observations, the antenna performs well. However, it is discovered that differences between simulated and measured results are caused by fabrication faults and unavoidable cable losses. Additionally, these measurement techniques are not the most trustworthy ones for measuring small antennas, particularly in the millimeter wave frequency region. Between simulated and measured findings, there might be a difference because of how the measuring technology affects the results. The procedure outlined here is utilized to use a far-field measurement instrument to gauge the suggested antenna design's radiation patterns in an echoless space. Although the antenna has good modeling and measurement performance, it is highlighted that there may be inconsistencies due to fabrication issues, cable losses, and the inherent limits of the measuring instrument. This is a classic antenna design challenge, particularly in higher-frequency bands like mm-wave.

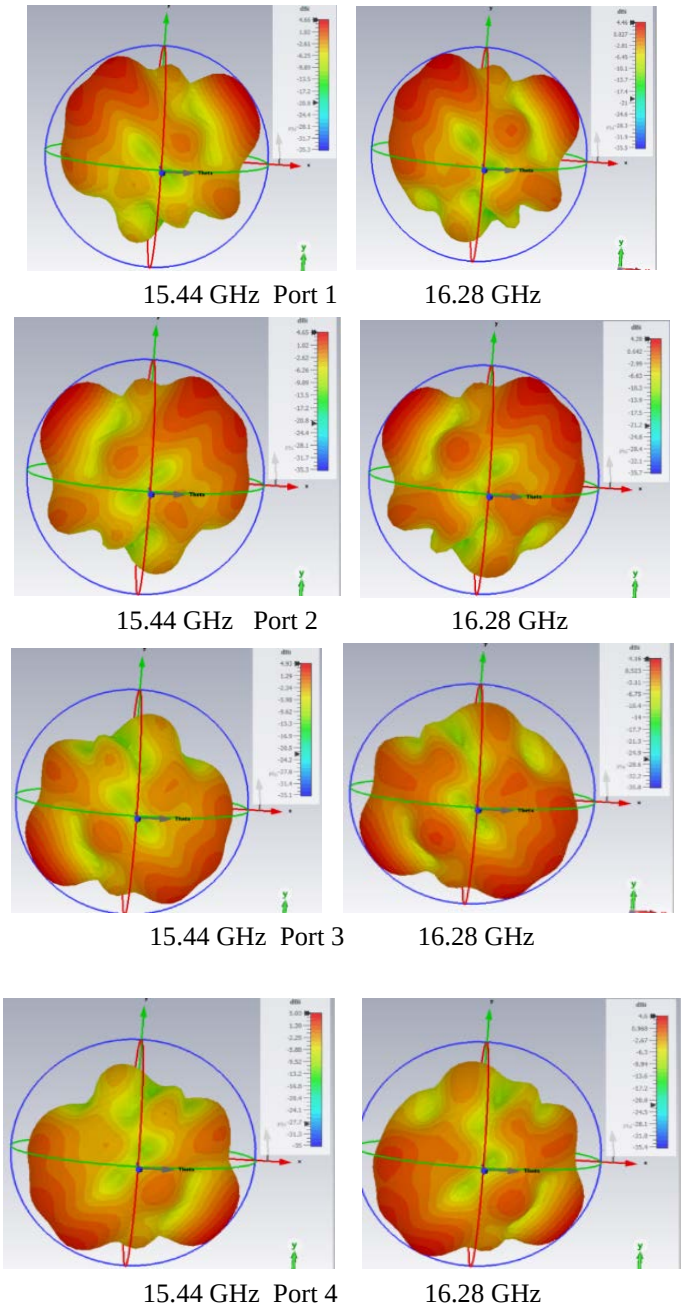

Figure 5. The Designed Antenna (simulated) Radiation Characteristics

DGS incorporation: Incorporating a Defect in the Ground Structure improves the designed antenna system's performance and bandwidth. The MIMO antennas with DGS now cover the operating range between 13 to 17.7 GHz, according to the reflection coefficient curves for this equipment. This shows a substantial improvement in the antenna system's ability to function at a range of frequencies. 5.03 dBi is the highest observed gain for Ant.4 at port 4.

Maximum Bandwidth: By adding the DGS and switching the MIMO antenna system from two to four ports, the maximum bandwidth was increased to 13 to 17.7 GHz. The antenna can support a variety of applications and communication protocols

because of its broad frequency range. Figure 3's research and results show how the performance of the antenna system increased from a simple design to an optimized MIMO array. The antenna's bandwidth and coverage over the millimeter-wave frequency range have been considerably enhanced by the incorporation of DGS and the expansion of the array's element count.

CONCLUSIONS

A four-port MIMO antenna for 5G mm-wave and IoT applications was presented. The designed design includes a multiple-component high-gain antenna array with extended operating bands for each MIMO antenna. The operational frequency range spans from 14.2 GHz to 16.8 GHz. 5.03 dBi is also the design's observed peak gain. With quick, efficient networking, AI applications will be able to process enormous amounts of data more quickly and efficiently. For instance, if a nearby apartment tower opens, smart city AI may automatically correlate traffic signal data and adopt new patterns. The automatic detection of potential security breaches or unauthorized visitors is made possible by smart security and machine vision. By easing the transmission of data from devices to the main cloud to train or improve AI models, 5G will aid in enabling AI inference at the edge. For instance, real-world data on road conditions obtained by connected automobiles can improve cloud-based mapping systems. High-frequency bands, or FR2, are millimeter waves with frequencies of 6 GHz or higher. They are larger bands for 5G. There are accessible surplus spectrum resources in FR2.

CONFLICT OF INTEREST

The authors declared no conflict of interest there for publication of this work.

REFERENCES

1. 5g Spectrum GSMA Public Policy Position. Available online: https://www.gsma.com/latinamerica/wp-content/uploads/2019/03/5G-Spectrum-Positions.pdf (accessed on 23 April **2019**).
2. 5g Spectrum Auction Picks up in 2018—Report by Gsa. Available online: https://www.telecomlead.com/5g/5g-spectrum-auction-picks-up-in-2018-report-by-gsa-88154 (accessed on 23 April **2019**).
3. Y. Yashchyshyn, K. Derzakowski, G. Bogdan, et al. 28 GHz Switched-Beam Antenna Based on S-PIN Diodes for 5G Mobile Communications. *IEEE Antennas Wirel. Propag. Lett.* **2018**, 17 (2), 225–228.
4. M.C. Tang, T. Shi, R.W. Ziolkowski. A Study of 28 GHz, Planar, Multilayered, Electrically Small, Broadside Radiating, Huygens Source Antennas. *IEEE Trans. Antennas Propag.* **2017**, 65 (12), 6345–6354.
5. X. Lin, B.C. Seet, F. Joseph, E. Li. Flexible Fractal Electromagnetic Bandgap for Millimeter-Wave Wearable Antennas. *IEEE Antennas Wirel. Propag. Lett.* **2018**, 17 (7), 1281–1285.
6. R.N. Akhtar, A.A. Deshpande, A.K. Kureshi. Defected Top diamond shaped Patch Antenna for Multi-band operations. *J. Integr. Sci. Technol.* **2021**, 9 (2), 98–106.
7. S.X. Ta, H. Choo, I. Park. Broadband Printed-Dipole Antenna and Its Arrays for 5G Applications. *IEEE Antennas Wirel. Propag. Lett.* **2017**, 16, 2183–2186.
8. J. Kim, S.C. Song, H. Shin, Y.B. Park. Radiation from a millimeter-wave rectangular waveguide slot array antenna enclosed by a Von Karman radome. *J. Electromagn. Eng. Sci*. **2018**, 18 (3), 154–159.
9. P.A. Dzagbletey, Y.B. Jung. Stacked microstrip linear array for millimeter-wave 5G baseband communication. *IEEE Antennas Wirel. Propag. Lett.* **2018**, 17 (5), 780–783.
10. M. Khalily, R. Tafazolli, P. Xiao, A.A. Kishk. Broadband mm-Wave Microstrip Array Antenna with Improved Radiation Characteristics for Different 5G Applications. *IEEE Trans. Antennas Propag.* **2018**, 66 (9), 4641–4647.
11. S. Zhu, H. Liu, Z. Chen, P. Wen. A compact gain-enhanced vivaldi antenna array with suppressed mutual coupling for 5G mmwave application. *IEEE Antennas Wirel. Propag. Lett.* **2018**, 17 (5), 776–779.
12. Z. Briqech, A.R. Sebak, T.A. Denidni. Low-Cost Wideband mm-Wave Phased Array Using the Piezoelectric Transducer for 5G Applications. *IEEE Trans. Antennas Propag.* **2017**, 65 (12), 6403–6412.
13. B. Yu, K. Yang, C.Y.D. Sim, G. Yang. A Novel 28 GHz Beam Steering Array for 5G Mobile Device with Metallic Casing Application. *IEEE Trans. Antennas Propag.* **2018**, 66 (1), 462–466.
14. J. Bang, J. Choi. A SAR reduced mm-wave beam-steerable array antenna with dual-mode operation for fully metal-covered 5G cellular handsets. *IEEE Antennas Wirel. Propag. Lett.* **2018**, 17 (6), 1118–1122.
15. M. Ikram, Y. Wang, M.S. Sharawi, A. Abbosh. A novel connected PIFA array with MIMO configuration for 5G mobile applications. In *2018 Australian Microwave Symposium, AMS 2018 - Conference Proceedings*; Brisbane, Australia, **2018**; Vol. 2018-January, pp 19–20.
16. M.K. Pote, P. Mukherji, A. Sonawane. Design of 5G Microstrip patch array antenna for gain enhancement. *J. Integr. Sci. Technol.* **2022**, 10 (3), 198–203.
17. K. Dutt, D.S. Sodha. Multiband frequency switchable Microstrip antenna design for satellite application. *J. Integr. Sci. Technol*. **2022**, 10 (3), 189–192.
18. Y. Sun, K.W. Leung. Substrate-Integrated Two-Port Dual-Frequency Antenna. *IEEE Trans. Antennas Propag.* **2016**, 64, 3692–3697.
19. M.S. Sharawi, S.K. Podilchak, M.T. Hussain, Y.M.M. Antar. Dielectric resonator based MIMO antenna system enabling millimeter-wave mobile devices. *IET Microw. Antennas Propag.* **2017**, 11, 287–293.
20. B. Yang, Z. Yu, Y. Dong, J. Zhou, W. Hong. Compact Tapered Slot Antenna Array for 5G Millimeter-Wave Massive MIMO Systems. *IEEE Trans. Antennas Propag.* **2017**, 65, 6721–6727.
21. S.F. Jilani, A. Alomainy. Millimetre-wave T-shaped MIMO antenna with defected ground structures for 5G cellular networks. IET Microw. *Antennas Propag.* **2018**, 12, 672–677.
22. N. Shoaib, S. Shoaib, R.Y. Khattak, I. Shoaib, X. Chen, A. Perwaiz. MIMO Antennas for Smart 5G Devices. *IEEE Access* **2018**, 6, 77014–77021.
23. A.A.R. Saad, H.A. Mohamed. Printed millimeter-wave MIMO-based slot antenna arrays for 5G networks. *AEU Int. J. Electron. Commun*. **2019**, 99, 59–69.
24. H. Jiang, L. Si, W. Hu, X. Lv. A Symmetrical Dual-Beam Bowtie Antenna with Gain Enhancement Using Metamaterial for 5G MIMO Applications. *IEEE Photonics J*. **2019**, 11, 1–9.
25. N. Hussain, M. Jeong, J. Park, N. Kim. A Broadband Circularly Polarized Fabry-Perot Resonant Antenna Using A Single-Layered PRS for 5G MIMO Applications. *IEEE Access* **2019**, 7, 42897–42907.
26. Y. Zhang, J. Deng, M. Li, D. Sun, L. Guo. A MIMO Dielectric Resonator Antenna with Improved Isolation for 5G mm-Wave Applications. *IEEE Antennas Wirel. Propag. Lett*. **2019**, 18, 747–751.
27. R. Pandey, A.K. Shankhwar, A. Singh, An Improved Conversion Efficiency of 1.975 to 4.744GHz Rectenna for Wireless Sensor Applications. *Progress Electromagnetics Res. C*, **2021**, Vol. 109, 217–225.
28. S. Nandedkar, S. Nawale. Frequency and space diverse MIMO antenna with enhanced gain. *J. Integr. Sci. Technol.*, **2023**, 11(2), 482.